



HAL
open science

[C II] emission in z similar to 6 strongly lensed, star-forming galaxies

Kirsten K. Knudsen, Johan Richard, Jean-Paul Kneib, Mathilde Jauzac,
Benjamin Clément, Guillaume Drouart, Eiichi Egami, Lukas Lindroos

► **To cite this version:**

Kirsten K. Knudsen, Johan Richard, Jean-Paul Kneib, Mathilde Jauzac, Benjamin Clément, et al..
[C II] emission in z similar to 6 strongly lensed, star-forming galaxies. Monthly Notices of the Royal
Astronomical Society, 2016, 462 (1), pp.L6–L10. 10.1093/mnrasl/slw114 . hal-01440696

HAL Id: hal-01440696

<https://hal.science/hal-01440696>

Submitted on 14 Jan 2022

HAL is a multi-disciplinary open access archive for the deposit and dissemination of scientific research documents, whether they are published or not. The documents may come from teaching and research institutions in France or abroad, or from public or private research centers.

L'archive ouverte pluridisciplinaire **HAL**, est destinée au dépôt et à la diffusion de documents scientifiques de niveau recherche, publiés ou non, émanant des établissements d'enseignement et de recherche français ou étrangers, des laboratoires publics ou privés.



Distributed under a Creative Commons Attribution 4.0 International License

[C II] emission in $z \sim 6$ strongly lensed, star-forming galaxies

Kirsten K. Knudsen,¹★ Johan Richard,² Jean-Paul Kneib,^{3,4} Mathilde Jauzac,^{5,6,7}
Benjamin Clément,² Guillaume Drouart,⁸ Eiichi Egami⁹ and Lukas Lindroos¹

¹Department of Earth and Space Sciences, Chalmers University of Technology, Onsala Space Observatory, SE-43992 Onsala, Sweden

²Univ Lyon, Univ Lyon1, Ens de Lyon, CNRS, Centre de Recherche Astrophysique de Lyon UMR5574, F-69230, Saint-Genis-Laval, France

³Laboratoire d'Astrophysique, Ecole Polytechnique Fédérale de Lausanne (EPFL), Observatoire de Sauverny, CH-1290 Versoix, Switzerland

⁴Aix Marseille Université, CNRS, LAM (Laboratoire d'Astrophysique de Marseille), UMR 7326, F-13388 Marseille, France

⁵Centre for Extragalactic Astronomy, Department of Physics, Durham University, Durham DH1 3LE, UK

⁶Institute for Computational Cosmology, Durham University, South Road, Durham DH1 3LE, UK

⁷Astrophysics and Cosmology Research Unit, School of Mathematical Sciences, University of KwaZulu-Natal, Durban 4041, South Africa

⁸International Centre for Radio Astronomy Research, Curtin University, Bentley, WA6102, Perth, Australia

⁹Steward Observatory, University of Arizona, 933 N. Cherry Ave, Tucson, AZ 85721, USA

Accepted 2016 June 7. Received 2016 June 7; in original form 2016 March 4

ABSTRACT

The far-infrared fine-structure line [C II] at 1900.5 GHz is known to be one of the brightest cooling lines in local galaxies, and therefore it has been suggested to be an efficient tracer for star formation in very high redshift galaxies. However, recent results for galaxies at $z > 6$ have yielded numerous non-detections in star-forming galaxies, except for quasars and submillimetre galaxies. We report the results of ALMA observations of two lensed, star-forming galaxies at $z = 6.029$ and $z = 6.703$. The galaxy A383-5.1 (star formation rate [SFR] of $3.2 M_{\odot} \text{ yr}^{-1}$ and magnification of $\mu = 11.4 \pm 1.9$) shows a line detection with $L_{[\text{C II}]} = 8.9 \times 10^6 L_{\odot}$, making it the lowest $L_{[\text{C II}]}$ detection at $z > 6$. For MS0451-H (SFR = $0.4 M_{\odot} \text{ yr}^{-1}$ and $\mu = 100 \pm 20$) we provide an upper limit of $L_{[\text{C II}]} < 3 \times 10^5 L_{\odot}$, which is 1 dex below the local SFR– $L_{[\text{C II}]}$ relations. The results are consistent with predictions for low-metallicity galaxies at $z > 6$; however, other effects could also play a role in terms of decreasing $L_{[\text{C II}]}$. The detection of A383-5.1 is encouraging and suggests that detections are possible, but much fainter than initially predicted.

Key words: galaxies: evolution – galaxies: formation – galaxies: high-redshift – galaxies: ISM – submillimetre: galaxies.

1 INTRODUCTION

During the past decade, the number of galaxies with measured redshifts $z > 6$ has increased significantly (e.g. Hu et al. 2002; Iye et al. 2006) with even a few spectroscopic redshifts of $z > 7$ (Vanzella et al. 2011; Ono et al. 2012; Schenker et al. 2012; Shibuya et al. 2012; Finkelstein et al. 2013; Oesch et al. 2015; Watson et al. 2015; Zitrin et al. 2015), demonstrating the tremendous potential for progress of our understanding of galaxy formation during the first billion years after the big bang. There is an even larger number of galaxies with photometric redshifts $z > 6$ (e.g. McLure et al. 2013; Smit et al. 2015); however, spectroscopic redshifts are essential for studying the physical properties of the interstellar medium and the gas that fuels the star formation. Because of the intrinsic high luminosity and the large gas masses, several starburst and quasar host galaxies have been studied in great detail at $z > 6$ (e.g.

Maiolino et al. 2005; Venemans et al. 2012, 2016; Riechers et al. 2013; Wang et al. 2013; Bañados et al. 2015; Cicone et al. 2015; Willott, Bergeron & Omont 2015a). Such galaxies are interesting to understand the evolution of the most massive galaxies but are not representative of the overall galaxy population.

Various tracers are used for determining the properties of the gas in star-forming galaxies. In terms of studying molecular gas, CO is most commonly used as it is the second most abundant molecule and with bright emission lines from the rotational transitions that are visible in the (sub-)mm bands. One of the brightest lines seen in the far-infrared (FIR) in local star-forming galaxies is the fine-structure (FS) line [C II] (${}^2P_{3/2} \rightarrow {}^2P_{1/2}$) at 1900.537 GHz, which is found to correlate with the star formation rate (e.g. De Looze et al. 2014; Sargsyan et al. 2014). While local studies of the FIR FS lines are difficult due to the opacity of the Earth's atmosphere, at high z the lines are shifted towards the (sub-)mm bands and thus observable with ground-based telescopes.

With the increased ground-based capabilities of mm-wavelength telescopes, it has become possible to search for the [C II] line in less

* E-mail: kraiberg@chalmers.se

extreme galaxies at $z > 6$. However, a clear picture of this line as a tracer of the star formation is not emerging. Recently, Capak et al. (2015) and Willott et al. (2015b) detected [C II] in bright Lyman-break galaxies (LBG) at $5 < z < 6$ and $z \sim 6.1$, respectively, with the [C II] line luminosities and SFR following similar relations as those found for local star-forming galaxies. The galaxies are UV-luminous ($1-4L^*$; we use L^* for the corresponding redshift), representing the bright end of the UV-luminosity function. Maiolino et al. (2015) targeted three LBGs within the redshift range $z = 6.8-7.1$, but did not detect the [C II] line despite the galaxies having estimated SFRs $\sim 5-15 M_{\odot} \text{ yr}^{-1}$. However, they find a detection that is offset from one of the targets possibly explained by feedback and/or gas accretion. Similarly, Schaerer et al. (2015) obtained upper limits for two other LBGs at $z \sim 6.5-7.5$, of which one is lensed and with sub- L^* luminosity. Ly α emitting galaxies have been observed, including the massive Ly α -blob ‘Himiko’, however, no confirmed detection has so far been obtained (e.g. Kanekar et al. 2013; Ouchi et al. 2013; González-López et al. 2014; Ota et al. 2014). Almost all of these galaxies have non-detections in the FIR continuum suggesting a low dust-mass. Watson et al. (2015) found a clear detection of dust emission from a spectroscopically confirmed $z = 7.5$ galaxy, however, did not detect an expected bright [C II] line in the frequency range covered. The galaxy is strongly lensed by a magnification factor of 9.5, thus providing constraints on a sub- L^* galaxy.

In this letter we present ALMA observations of [C II] for two sub- L^* galaxies at $z > 6$. The two sources are A383-5.1 ($z = 6.027$) and MS0451-H ($z = 6.703$), which have estimated SFRs of 3.2 and $0.4 M_{\odot} \text{ yr}^{-1}$, respectively, and estimated magnification factors of $\mu = 11.4 \pm 1.9$ and 100 ± 20 , respectively (Richard et al. 2011; Stark et al. 2015, Kneib et al., in preparation). The strong lensing of both galaxies enables us to probe intrinsically fainter luminosities and SFR than previous observations. We assume a Λ CDM cosmology with $H_0 = 67.3 \text{ km s}^{-1} \text{ Mpc}^{-1}$, $\Omega_M = 0.315$, and $\Omega_{\Lambda} = 0.685$ (Planck Collaboration XVI et al. 2014).

2 OBSERVATIONS

We observed the sources MS0451-H and A383-5.1 with ALMA in Cycle-2. The observations were carried out in 2014 December and 2015 January and May. A separate receiver setup was used for each source tuning to the redshifted [C II] line; for A383 at $z = 6.027^1$ the central frequency was 270.462 GHz and for MS0451-H at $z = 6.703$ it was 246.727 GHz. The correlator was used in the frequency domain mode with one spectral window (spw) having a bandwidth of 1.875 GHz centred on the aforementioned frequencies, and the three other available spw’s used a continuum setup with a bandwidth of 2 GHz each distributed over 128 channels. The telescope configuration has baselines extending between 15 and 350 m for MS0451-H and 15 to 540 m for A383-5.1; the observations include baselines longer than initially proposed for. The integration time was 1.9 h for MS0451-H and 4.6 h for A383-5.1. Table 1 summarizes the details of the observations including a list of the calibrators.

Reduction, calibration, and imaging were done using CASA (Common Astronomy Software Application;² McMullin et al. 2007). The pipeline reduced data delivered from the observatory were of sufficient quality; no additional flagging and further calibration was

¹ The setup for A383-5.1 was based on the redshift from Richard et al. (2011), the redshift was revised to 6.029 following observations of the counter-image A383-5.2 (Stark et al. 2015).

² <https://casa.nrao.edu>

Table 1. Summary of the ALMA observations.

Date	N_{ant}	Calibrators		
		Flux	Bandpass	Gain
<i>MS0451-H</i>				
10-12-2014	37	J0423-013	J0423-0120	J0501-0159
26-12-2014	40	Uranus	J0338-4008	J0501-0159
26-12-2014	40	Uranus	J0423-013	J0501-0159
<i>A383-5.1</i>				
31-12-2014	36	J0423-013	J0423-0120	J0239-0234
14-01-2015	38	Uranus	J0423-013	J0239-0234
17-01-2015	35	Uranus	J0224+0659	J0239-0234
23-05-2015	34	J0238+166	J0423-013	J0239-0234
23-05-2015	34	J0423-013	J0423-013	J0239-0234
24-05-2015	34	J0238+166	J0224+0659	J0239-0234
24-05-2015	34	J0238+166	J0423-013	J0239-0234

necessary. The pipeline includes the steps required for standard reduction and calibration, such as flagging, bandpass calibration, as well as flux and gain calibration. A conservative estimate of the absolute flux calibration is 10 per cent. In the case of A383-5.1, a continuum source, flux density ~ 2 mJy, is seen 11 arcsec south of the point centre. We attempted to self-calibrate using this relatively bright source; however, this did not significantly improve the sensitivity.

The data were imaged both as continuum and spectral cube using natural weighting. A continuum image was produced combining all spectral windows, while a spectral cube was constructed for the spectral window tuned to the redshifted [C II] line. The obtained resolution is $0.86 \times 0.67 \text{ arcsec}^2 \text{ PA} = 94^\circ$ for A383-5.1 and $1.6 \times 0.9 \text{ arcsec}^2 \text{ PA} = 84^\circ$, and in both cases the rms is $11 \mu\text{Jy beam}^{-1}$. The rms in a 15.6 MHz channel near the redshifted line is $0.125 \text{ mJy beam}^{-1}$ and $0.163 \text{ mJy beam}^{-1}$ for A383-5.1 and MS0451-H, respectively.

3 RESULTS

In case of A383-5.1 we detect the redshifted [C II] line. The spectrum is shown in Fig. 1 together with an image of the integrated line overlaid on a near-infrared *HST* F140W image from the CLASH survey (Postman et al. 2012).³ We fit a Gaussian line profile to the extracted spectrum and use this to derive the line properties. The resulting fit parameters are: central frequency $\nu = 270.4448 \pm 0.0061 \text{ GHz}$, peak flux of $S_{\text{peak}} = 0.96 \pm 0.19 \text{ mJy}$, and full width at half-maximum linewidth of $\Delta V = 100 \pm 23 \text{ km s}^{-1}$. This corresponds to an integrated line intensity $I_{[\text{C II}]} = 0.102 \pm 0.032 \text{ Jy km s}^{-1}$ (including the flux uncertainty added in quadrature). We derive a redshift of $z_{[\text{C II}]} = 6.0274 \pm 0.0002$, which is in agreement with the optical/UV redshift of 6.029 ± 0.002 (Richard et al. 2011) and the C III] redshift of 6.0265 ± 0.00013 (Stark et al. 2015). We note the spectrum has been extracted from a data cube, which was imaged using natural weighting and tapering with 2D Gaussian with a corresponding 1 arcsec width as the source appears to be marginally extended. Using the uv -data of collapsed spectral channels around the peak of the emission line, we estimate the size of the source to be $\sim 0.16 \text{ arcsec}$ assuming a 2D Gaussian brightness distribution; however, due to the modest signal-to-noise ratio it is difficult to accurately measure its extent. The continuum is not detected, and we place a 5σ upper level $55 \mu\text{Jy}$.

³ <https://archive.stsci.edu/prepds/clash/>

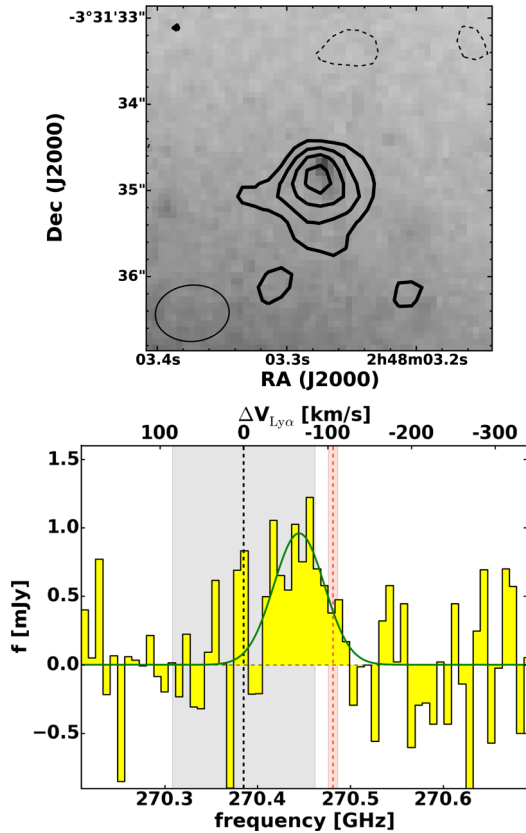


Figure 1. Top: *HST* WFC3 F140W image overlaid with the contours of the integrated spectral line. The contours show 2, 3, 4, 5 σ , and dashed show -2σ . The apparent gradient of NIR emission increasing from the lower part of the image is caused by the bright emission from the central galaxy of the A383 cluster. Bottom: ALMA spectra extracted at the position of A383-5.1 and centred at the frequency of the redshifted [C II] line. The green solid curve shows the best-fitting Gaussian. The vertical dashed line and grey area show the corresponding redshift and uncertainty determined from the Ly α line, and the red dashed line and area correspond to the redshift measured from C III] (Stark et al. 2015). The top-axis shows the velocity relative the Ly α redshift.

In the field around A383-5.1 we also detect two continuum sources, at 02:48:03.4, $-03:31:44.86$ with a flux of 2.2 mJy, and at 02:48:02.8, $-03:31:27.67$, integrated flux of 0.25 mJy, and an estimated source size of 2.4×1.1 arcsec² PA = 60°. The former is associated with the cD galaxy of the cluster ($z = 0.188$), and the latter is associated with a spiral galaxy at $z = 0.65$ (denoted as B18 in Smith et al. 2001).

For MS0451-H, we do not detect a line, and in Fig. 2 we show the extracted spectrum from the region corresponding to the near-infrared (NIR) source; as for A383-5.1, the spectrum was extracted from a cube that was imaged using natural weighting and tapering. We measure a rms of 0.05 mJy beam⁻¹ for a channel of 100 km s⁻¹. Assuming this corresponds to the full width at half-maximum width of the line, we estimate a 5 σ upper limit of 0.026 Jy km s⁻¹. We do not detect the continuum and place an upper limit of 55 μ Jy.

We estimate the [C II] line luminosity using $L_{[\text{C II}]} = 1.04 \times 10^{-3} S \Delta V D_L^2 \nu_{\text{obs}}$ (e.g. Solomon & Vanden Bout 2005; Carilli & Walter 2013). De Looze et al. (2014) have investigated the [C II] line as a SFR estimator for local star-forming galaxies against other probes and for different classes of galaxies. We use the relation for low-metallicity galaxies to estimate the SFR from $L_{[\text{C II}]}$ under the

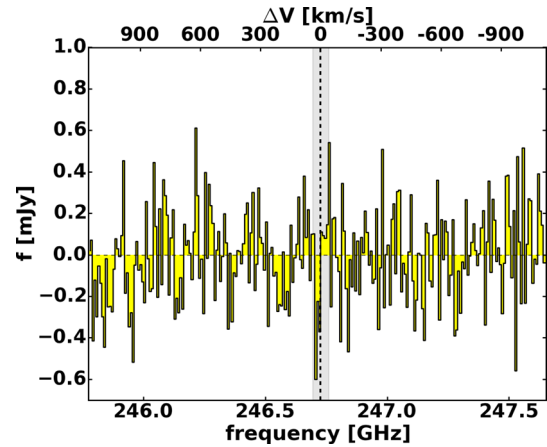


Figure 2. The ALMA band-6 spectrum extracted at the position of the MS0451-H arc. The vertical line and grey area indicate the corresponding redshift and uncertainty determined from the Ly α line. The top-axis shows the velocity relative the Ly α redshift.

assumption that the [C II] line traces star formation in the galaxies. Furthermore, we use the continuum upper limit to estimate the FIR luminosity upper limits assuming a modified blackbody spectrum with a temperature $T = 35$ K and $\beta = 1.6$ (e.g. Rémy-Ruyer et al. 2013). For comparison with the SFR derived from the optical/NIR observations, we estimate a SFR from the L_{IR} assuming a Chabrier IMF (e.g. Carilli & Walter 2013). We correct the values for the estimated gravitational magnification (Richard et al. 2011, Kneib et al., in preparation). Results and upper limits are summarized in Table 2. We note that the CMB temperature is 19.1 and 21 K for $z = 6.027$ and $z = 6.703$, respectively. Following the analysis of da Cunha et al. (2013), we estimate that the CMB heating would increase the temperature by less than a per cent for the assumed values and that about 14–20 per cent of the intrinsic continuum flux density would be missed due to the CMB background emission.

4 DISCUSSION

A383-5.1 has the lowest [C II] luminosity among all detections of this line at $z > 6$, and the upper limit for MS0451-H is more than 1.5 dex below other upper limits. Both galaxies are selected as UV-bright, star-forming, and with gravitational magnification > 10 . The latter enabled us to do deeper observations than previously presented and thus probe towards SFRs and stellar masses comparable to the low-mass end and less extreme systems. In Fig. 3 we show the results together with results for other high- z and local galaxies.

Using combined stellar population synthesis modelling and photoionization modelling of the gas-component, Stark et al. (2015) find that the metallicity is $\log(Z/Z_{\odot}) = -1.33$ for A383-5.1. This relatively low metallicity is comparable to the metallicity found in some nearby dwarf galaxies. The line luminosity for A383-5.1, as well as the MS0451-H upper limit and the IR luminosity limits, is similar to nearby, low- Z dwarfs. Using *Herschel* PACS spectroscopy, Cormier et al. (2015) studied the properties of FIR FS lines, including the [C II] line, of the low- Z ISM of dwarf galaxies. The $L_{[\text{C II}]} / L_{\text{IR}}$ ratio has a large scatter for dwarf galaxies, and the lowest metallicity systems, $Z/Z_{\odot} < 1/20$, agree with that scatter. Based on the $L_{[\text{C II}]}$ of A383-5.1, assuming a ratio of 0.6 per cent and 0.06 per cent, we estimate $L_{\text{IR}} \sim 1.4\text{--}14 \times 10^9 L_{\odot}$. This is partly in agreement with the lower limit on the $L_{[\text{C II}]} - L_{\text{FIR}}$ ratio derived from our results (see Table 2), suggesting that the [C II] line contributes

Table 2. Resulting properties for A383-5.1 and MS0451-H together with UV-optical estimates.

Name	$z_{\text{Ly}\alpha}$	$z_{[\text{C II}]}$	μ	$L_{[\text{C II}]}$ [L_{\odot}]	SFR $_{[\text{C II}]}$ [$M_{\odot} \text{ yr}^{-1}$]	L_{IR} [L_{\odot}]	SFR $_{\text{IR}}$ [$M_{\odot} \text{ yr}^{-1}$]	SFR $_{\text{optical}}$ [$M_{\odot} \text{ yr}^{-1}$]
A383-5.1	6.029 ± 0.002	6.0274 ± 0.0002	11.4 ± 1.9	$(8.9 \pm 3.1) \times 10^6$ ^a	0.68 ± 0.24	$<0.5 \times 10^{10}$	<0.5	3.2
MS0451-H	6.703 ± 0.001	...	100 ± 20	$<3.0 \times 10^{5b}$	<0.04	$<0.07 \times 10^{10}$	<0.07	0.4

^aThe error includes the uncertainties from the line fit, the flux calibration, and the uncertainty on the magnification.

^bAssuming a linewidth of 100 km s^{-1} as measured for A383-5.1

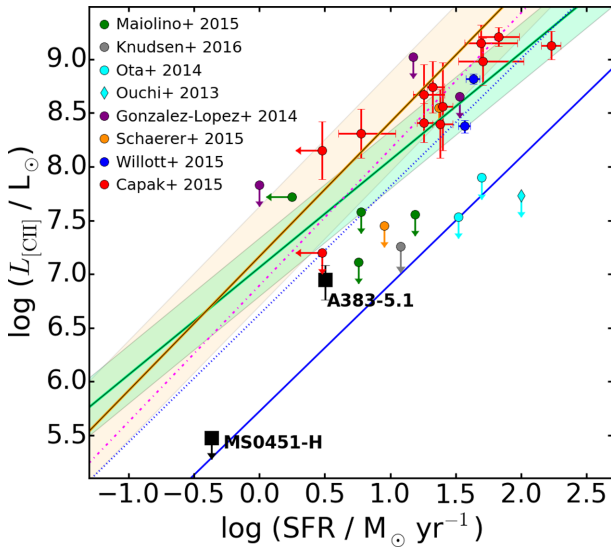


Figure 3. The [C II] line luminosity $L_{[\text{C II}]}$ versus star formation rate. Black squares show the detection A383-5.1 and the sensitive upper limit for MS0451-H (corrected for magnification). We also include the recent $z \sim 6$ results from Ouchi et al. (2013), Ota et al. (2014), González-López et al. (2014), Willott et al. (2015b), Maiolino et al. (2015), Capak et al. (2015), Schaerer et al. (2015), Knudsen et al. (2016). The $L_{[\text{C II}]}$ –SFR relation, where the green region shows the relation for local star-forming galaxies and the orange region shows that for low-metallicity dwarf galaxies (De Looze et al. 2014). The blue solid and dotted line shows the resulting relation from low-metallicity simulations (Vallini et al. 2015) (solid: $Z = 0.05 Z_{\odot}$, dotted: $Z = 0.2 Z_{\odot}$) and the magenta dash–dotted line the results for massive $z \sim 2$ galaxies (Olsen et al. 2015).

significantly to the cooling. For MS0451-H, we do not have an estimate for the metallicity given the limited optical (rest-frame UV) data available (Kneib et al., in preparation).

The sample from Capak et al. (2015) contains bright LBGs with luminosities $> L^*$ and in the redshift range $5 < z < 6$, and while this is below the redshift range that we are probing ($z > 6$), it is to date the largest sample of [C II] detections of galaxies that are not quasar host galaxies or SMGs. That sample is in reasonable agreement with the SFR– $L_{[\text{C II}]}$ relations seen for local galaxies (e.g. De Looze et al. 2014). Similarly, the two LBG detections from Willott et al. (2015b) also follow these relations. On the other hand, several [C II] searches towards both LAEs and LBGs have resulted in non-detections (Ouchi et al. 2013; Ota et al. 2014; González-López et al. 2014; Maiolino et al. 2015; Schaerer et al. 2015), where several observations provide upper limits below the local SFR– $L_{[\text{C II}]}$ comparable to our detection of A383-5.1.

With an excitation temperature of 91.2 K and the ionization potential of carbon of 11.2 eV, the [C II] is a good tracer of the dif-

fuse ISM, of the cold neutral medium (CNM) phase as well as of the photon-dominated regions (PDRs) caused by star formation in molecular clouds. Both models and observations of nearby galaxies show that [C II] emission is an efficient cooling line and that the line luminosity is correlated with the star-formation rate of galaxies (e.g. De Looze et al. 2014; Sargsyan et al. 2014); however, for IR bright starburst galaxies and AGN, the efficiency drops (e.g. Díaz-Santos et al. 2013).

It is unclear why so many $z > 6$ galaxies remain undetected, or, as in the case of A383-5.1, show a fainter than predicted [C II] line. It has been suggested that low metallicity is the main reason. As shown in PDR modelling, the [C II] line intensity decreases for lower metallicity, although not linearly (e.g. Röllig et al. 2006). Given that the [C II] line correlates well with the SFR for nearby, low-metallicity galaxies (e.g. De Looze et al. 2014), it would be expected that this is also the case for high- z low-metallicity galaxies. However, the [C II] deficit suggests that the physical conditions are very different from nearby low- Z galaxies. This [C II] deficit is different from the classical one found for FIR luminous galaxies (e.g. Luhman et al. 2003; Stacey et al. 2010). Aside from metallicity playing a role, other mechanisms could contribute, such as a harder radiation field which could further ionize the carbon into C^{++} ; in fact the spectral modelling of A383-5.2 (the counterimage) yields a high ionization parameter $\log U = 1.79$ (Stark et al. 2015). In such case, observations of e.g. C III] lines would reveal elevated ratios. Increased temperature of the ISM and PDRs would result in other FS lines being more efficient coolants and thus brighter than [C II]. For example, the [O III] 88 μm line is normally expected to be tracing H II regions rather than diffuse and clumpy inter-cloud medium (see e.g. Cormier et al. 2015, for further details). Further, we note that gas-phase carbon could be depleted on to carbonaceous dust grains.

In simulations of high- z galaxies, the recent study by Vallini et al. (2015) focused on differences arising when taking into account varying metallicity. Vallini et al. (2015) produce a metallicity-dependent relation for $L_{[\text{C II}]}$ –SFR based on a constant metallicity distribution throughout the simulated galaxy ($z = 6.6$). For low Z , $Z = 0.05$ – $0.2 Z_{\odot}$, the relation is below that of local galaxies. A383-5.1 has a metallicity similar to the low- Z assumption of the Vallini et al. (2015) model. The model results are consistent with our detection of A383-5.1, which suggests that metallicity plays an important role. However, given that we only have one detection and the remaining being non-detections, we cannot confirm this. We show the Vallini et al. model results in Fig. 3, and, for comparison, include the resulting relation from multi-phase ISM simulations of $z \sim 2$ massive galaxies by Olsen et al. (2015), which tends to follow the relations seen for local galaxies.

It is, however, important to also investigate the selection bias for high- z galaxies. The fact that Lyman α emitters, despite high estimates for SFR, remain undetected in the relatively deep ALMA

observations of the [C II] line could suggest that SFRs are overestimated and while the Ly α emission likely traces star formation, a fraction of it could be powered by other mechanisms, such as shocks of gas inflow.

To summarize, while it has been suggested that [C II] would be a relatively bright tracer for star formation in high- z galaxies – and with the advantage of being redshifted into the ~ 1 mm wavelength range – the recent results show that the line luminosity does not follow the same correlations as local galaxies. With the A383-5.1 detection, we find that it is possible to detect [C II] towards $z > 6$ star-forming galaxies, although the line luminosity is lower than predicted from local galaxies and also from high- z SMGs and QSO hosts. This implies that future observations have the potential to yield detections, although the predicted line flux will likely be lower than when derived from local relations, even when using local low- z relations.

ACKNOWLEDGEMENTS

We thank the staff of the Nordic ALMA Regional Center node for their support and helpful discussions. We thank the referee for useful comments. KK acknowledges support from the Swedish Research Council (grant: 621-2011-5372) and the Knut and Alice Wallenberg Foundation. JR acknowledges support from the ERC starting grant CALENDs (336736). JPK acknowledges support from the ERC advanced grant LIDA and from CNRS. MJ is supported by the Science and Technology Facilities Council [grant number ST/L00075X/1 & ST/F001166/1]. This paper makes use of the following ALMA data: ADS/JAO.ALMA#2013.1.01241.S. ALMA is a partnership of ESO (representing its member states), NSF (USA) and NINS (Japan), together with NRC (Canada) and NSC and ASIAA (Taiwan) and KASI (Republic of Korea), in cooperation with the Republic of Chile. The Joint ALMA Observatory is operated by ESO, AUI/NRAO and NAOJ.

REFERENCES

- Bañados E., Decarli R., Walter F., Venemans B. P., Farina E. P., Fan X., 2015, *ApJ*, 805, L8
- Capak P. L. et al., 2015, *Nature*, 522, 455
- Carilli C. L., Walter F., 2013, *ARA&A*, 51, 105
- Cicone C. et al., 2015, *A&A*, 574, A14
- Cormier D. et al., 2015, *A&A*, 578, A53
- da Cunha E. et al., 2013, *ApJ*, 765, 9
- De Looze I. et al., 2014, *A&A*, 568, A62
- Díaz-Santos T. et al., 2013, *ApJ*, 774, 68
- Finkelstein S. L. et al., 2013, *Nature*, 502, 524
- González-López J. et al., 2014, *ApJ*, 784, 99
- Hu E. M., Cowie L. L., McMahon R. G., Capak P., Iwamuro F., Kneib J.-P., Maihara T., Motohara K., 2002, *ApJ*, 568, L75
- Iye M. et al., 2006, *Nature*, 443, 186
- Kanekar N., Wagg J., Ram Chary R., Carilli C. L., 2013, *ApJ*, 771, L20
- Knudsen K. K., Watson D., Frayer D., Christensen L., Gallazzi A., Michałowski M. J., Richard J., Zavala J., 2016, *MNRAS*, preprint ([arXiv:1603.03222](https://arxiv.org/abs/1603.03222))
- Luhman M. L., Satyapal S., Fischer J., Wolfire M. G., Sturm E., Dudley C. C., Lutz D., Genzel R., 2003, *ApJ*, 594, 758
- Maiolino R. et al., 2005, *A&A*, 440, L51
- Maiolino R. et al., 2015, *MNRAS*, 452, 54
- McLure R. J. et al., 2013, *MNRAS*, 432, 2696
- McMullin J. P., Waters B., Schiebel D., Young W., Golap K., 2007, in Shaw R. A., Hill F., Bell D. J., eds, *Astronomical Society of the Pacific Conference Series Vol. 376, Astronomical Data Analysis Software and Systems XVI*. Astron. Soc. Pac., San Francisco, p. 127
- Oesch P. A. et al., 2015, *ApJ*, 804, L30
- Olsen K. P., Greve T. R., Narayanan D., Thompson R., Toft S., Brinch C., 2015, *ApJ*, 814, 76
- Ono Y. et al., 2012, *ApJ*, 744, 83
- Ota K. et al., 2014, *ApJ*, 792, 34
- Ouchi M. et al., 2013, *ApJ*, 778, 102
- Planck Collaboration XVI et al., 2014, *A&A*, 571, A16
- Postman M. et al., 2012, *ApJS*, 199, 25
- Rémy-Ruyer A. et al., 2013, *A&A*, 557, A95
- Richard J., Kneib J.-P., Ebeling H., Stark D. P., Egami E., Fiedler A. K., 2011, *MNRAS*, 414, L31
- Riechers D. A. et al., 2013, *Nature*, 496, 329
- Röllig M., Ossenkopf V., Jeyakumar S., Stutzki J., Sternberg A., 2006, *A&A*, 451, 917
- Sargsyan L., Samsonyan A., Lebouteiller V., Weedman D., Barry D., Bernard-Salas J., Houck J., Spoon H., 2014, *ApJ*, 790, 15
- Schaerer D., Boone F., Zamojski M., Staguhn J., Dessauges-Zavadsky M., Finkelstein S., Combes F., 2015, *A&A*, 574, A19
- Schenker M. A., Stark D. P., Ellis R. S., Robertson B. E., Dunlop J. S., McLure R. J., Kneib J.-P., Richard J., 2012, *ApJ*, 744, 179
- Shibuya T., Kashikawa N., Ota K., Iye M., Ouchi M., Furusawa H., Shimazaki K., Hattori T., 2012, *ApJ*, 752, 114
- Smit R. et al., 2015, *ApJ*, 801, 122
- Smith G. P., Kneib J.-P., Ebeling H., Czoske O., Smail I., 2001, *ApJ*, 552, 493
- Solomon P. M., Vanden Bout P. A., 2005, *ARA&A*, 43, 677
- Stacey G. J., Hailey-Dunsheath S., Ferkinhoff C., Nikola T., Parshley S. C., Benford D. J., Staguhn J. G., Fiolet N., 2010, *ApJ*, 724, 957
- Stark D. P. et al., 2015, *MNRAS*, 450, 1846
- Vallini L., Gallerani S., Ferrara A., Pallottini A., Yue B., 2015, *ApJ*, 813, 36
- Vanzella E. et al., 2011, *ApJ*, 730, L35
- Venemans B. P. et al., 2012, *ApJ*, 751, L25
- Venemans B. P., Walter F., Zschaechner L., Decarli R., De Rosa G., Findlay J. R., McMahon R. G., Sutherland W. J., 2016, *ApJ*, 816, 37
- Wang R. et al., 2013, *ApJ*, 773, 44
- Watson D., Christensen L., Knudsen K. K., Richard J., Gallazzi A., Michałowski M. J., 2015, *Nature*, 519, 327
- Willott C. J., Bergeron J., Omont A., 2015a, *ApJ*, 801, 123
- Willott C. J., Carilli C. L., Wagg J., Wang R., 2015b, *ApJ*, 807, 180
- Zitrin A. et al., 2015, *ApJ*, 810, L12

This paper has been typeset from a $\text{\TeX}/\text{\LaTeX}$ file prepared by the author.